MPRA
Munich Personal RePEc Archive

The Rice Market Reaction to El Nino Southern Oscillation Shocks

Ubilava, David and Valera, Harold Glenn and Pede, Valerien

School of Economics, University of Sydney, International Rice Research Institute

19 February 2022

Online at https://mpra.ub.uni-muenchen.de/123384/
MPRA Paper No. 123384, posted 19 Jan 2025 14:23 UTC

The Rice Market Reaction to El Nino Southern Oscillation Shocks

David Ubilava† *Harold Glenn Valera*‡ *Valerien O. Pede*‡

†School of Economics, University of Sydney

‡International Rice Research Institute

* Corresponding author. David Ubilava can be contacted at: david.ubilava@sydney.edu.au.

Abstract

We study the role of El Niño Southern Oscillation (ENSO) in the intermediate-term price dynamics of twenty rice varieties across six key rice-exporting countries over the 2011-2021 period. We apply two inter-related techniques. First, we generate impulse responses for up to 26-week horizons from linear projections to illustrate changes in rice price growth after ENSO shocks. Then, we assess the role of ENSO in predicting rice prices over the considered horizons. We find that ENSO shocks alter the dynamics of rice export prices from Thailand and, to a lesser extent, South America. In these regions, we also find that ENSO-related information facilitates the more accurate intermediate-term price forecasts. Since the price of Thai 5% long-grain white rice is considered the international price or the reference price, the fact that that ENSO shocks alter the price dynamics of rice varieties from Thailand suggests the susceptibility of international rice markets to ENSO shocks. Overall, our findings allude to the heterogeneity of the ENSO effect on rice markets and offer important insights for assessing the repercussions of climate change, which has been hypothesized to amplify ENSO cycles as well as the related weather repercussions in the usually affected regions.

Keywords: ENSO, Forecasting, Local Projections, Prices, Rice

JEL Codes: Q02, Q54, C53

---

[1] Version accepted for publication. 2211-9124 © 2024 International Rice Research Institute. Published by Elsevier B.V. Published in Global Food Security, 41, 2024, 100754. https://doi.org/10.1016/j.gfs.2024.100754.
Link: https://www.sciencedirect.com/science/article/pii/S2211912424000166

1. Introduction

Rice is arguably one the world's most affordable staple commodities. Much of it is produced in South and Southeast Asia and consumed around the world, thus emphasizing its role in achieving global poverty alleviation and food security (Takahashi and Barrett, 2014; Fan et al., 2005; Bandumula, 2018). This key rice-producing region also happens to be most susceptible to systemic weather shocks associated with El Niño Southern Oscillation (ENSO). Droughts associated with the El Niño phase of the ENSO cycle pose considerable risk to rice producers. This, in turn, impacts the availability and affordability of this commodity.[1] Previous studies have extensively investigated the availability of rice by estimating changes in crop production in response to climate shocks and weather variation (see, for example, Wang et al., 2022, as well as references cited therein). In this study we examine the role that ENSO shocks play in short-term rice price fluctuations, and in doing so we shed light on transitory changes in the affordability of rice.

Specifically, we examine the rice market reaction to ENSO shocks using two different but inter-related techniques. To begin, we apply the linear projections method of Jorda (2005) to illustrate rice price impulse responses in relation to ENSO shocks. The method lends itself to direct forecasting. So, we then assess the role of ENSO in predictability of rice prices in the short and intermediate run.

Rice is a heterogeneous commodity (Jamora and von Cramon-Taubadel, 2016; Koizumi and Furuhashi, 2020). The types and quality of rice produced in different countries vary considerably. For example, an aromatic rice variety, such as Basmati rice, is almost

[1] Here, *availability* refers to global rice supply through production and storage, and *affordability* refers to the price of rice.

exclusively produced in India and Pakistan, while a specialty rice variety, such as glutinous rice, is primarily produced in Thailand and other Southeast Asian countries. Although highly geographically concentrated, rice is not endemic to the South and Southeast Asian region. Other notable rice-producing countries include the United States, as well as several South American, African, and European countries. Considering varying types and quality of rice, ENSO shocks can have nontrivial impact on different rice markets. Our findings allude to it.

We study weekly prices of twenty rice varieties across six key rice-producing countries over the 2011-2021 period. For ENSO, we use weekly data on sea surface temperature anomalies in the Niño3.4 region (5^{o}N—5^{o}S, 120^{o}W—170^{o}W). We find that the effect of ENSO shocks is most evident in prices of rice varieties from Thailand and, to a lesser extent, South American countries. Specifically, a one standard deviation ENSO shock results in weekly 0.2 percent increase in the returns of Thailand rice varieties in the intermediate run. This effect is persistent, and over the course of four-to-twenty-week period it adds up to approximately two-to-four percent price increase, depending on the variety. In addition, ENSO-related information facilitates more accurate intermediate-term forecasting of rice prices from the affected regions. Specifically for Thailand rice, more accurate forecasts, due to ENSO, are achieved in white long-grain, parboiled, and white glutinous, but not in fragrant rice varieties.

This study provides several contributions to the literature. First, it uses an array of rice prices from different geographical regions that can be impacted by ENSO in different ways. In doing so, it addresses a heterogeneous effect ENSO shocks have on different rice markets. Second, it uses weekly data, thus unveiling dynamic linkages that may be camouflaged in temporally more aggregated price series.

While prices of rice varieties from across different countries have been studied previously, the research primarily focused on market integration and price transmission from global to local markets (e.g., John, 2013), as well as between the local markets (e.g., Chen and Saghaian, 2016) or across the rice varieties (e.g., Ghoshray, 2008; Chulaphan et al., 2013). These studies do not examine the effect of ENSO. Studies that do examine the role of ENSO on rice prices (e.g., Ubilava, 2018), primarily rely on a single reference-category rice variety, thus inherently neglecting any heterogeneity in the effect across regions and varieties.

The findings of this study enhance our understanding of rice price movement in response to ENSO shocks that tend to affect the key rice-producing countries once every several years. These findings will also offer important implications from the perspective of climate change, which is hypothesized to amplify ENSO cycles as well as the related weather repercussions in the usually affected regions. In what follows, we first describe the data used in the analysis as well as the empirical framework that help us address the research question. We then summarize the main results of this study, followed by the discussion of the results and their implications.

Data

We use weekly rice price data obtained from the Live Rice Index price database (available at https://livericeindex.com/). The data range the May 2011 – October 2021 months. From a large set of series, we retained the prices with no missing data or those with very few missing observations (less than two percent of the sample); in instances where the data were missing, we extrapolated the missing observations from the nearest past observed data-point, unless the observations at the beginning of the series were missing, in which case we extrapolated the missing data from the nearest future observed data-point. We discarded the series of highly correlated prices. As a result, for the analysis we retained 20 price series, which are featured in the top panel of Figure 1.

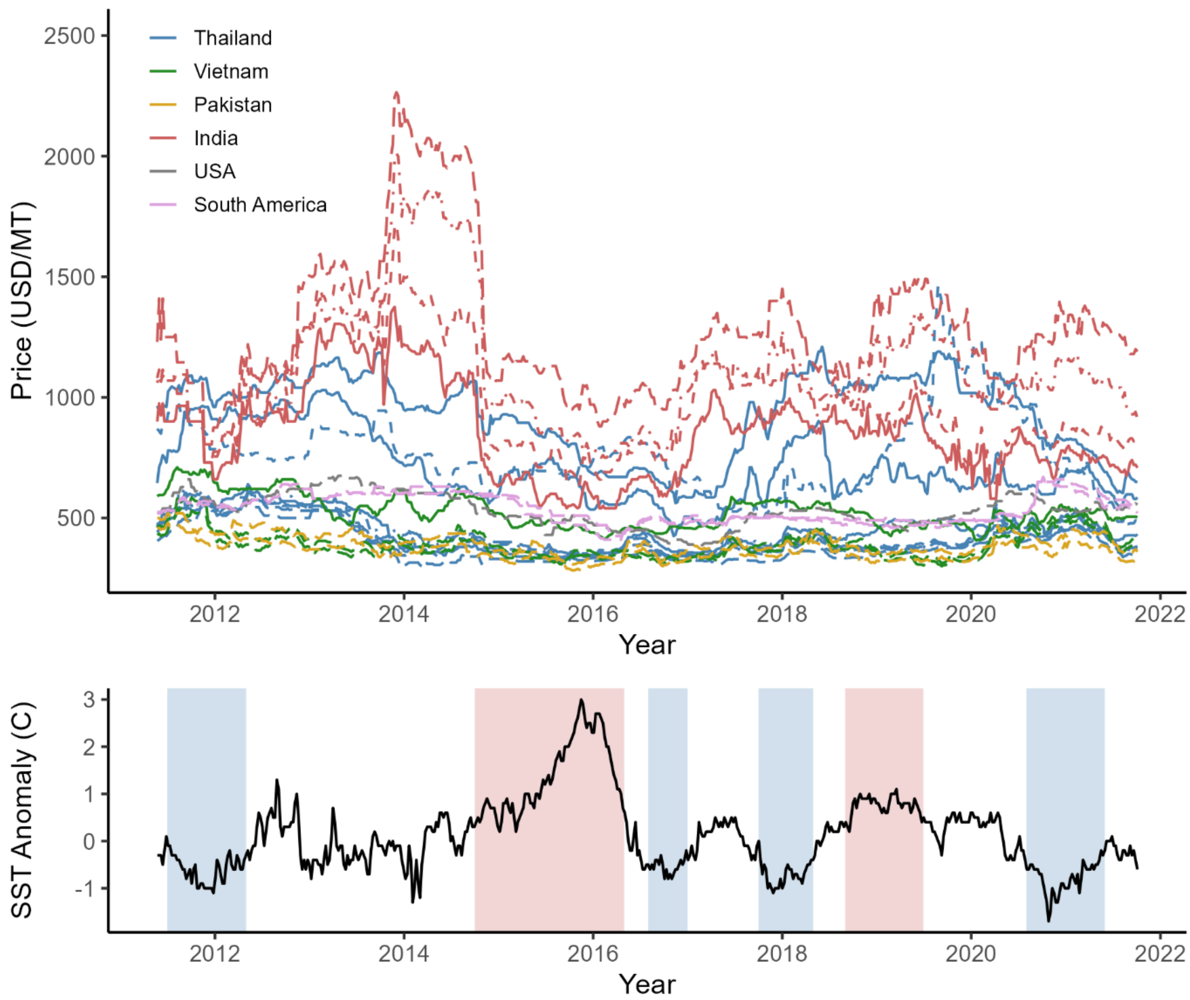

Figure 1: Rice Prices and ENSO.
Note: the top panel features weekly rice prices, from the Live Rice Index database (https://livericeindex.com/), and the bottom panel illustrates the sea surface anomaly in the Niño3.4 Pacific region along with periods of La Nina (shade of blue) and El Niño (shade of red) episodes, from the Climate Prediction Centre of the National Oceanic and Atmospheric Administration (https://www.cpc.ncep.noaa.gov/data/indices/). The line types indicate rice varieties (labels omitted for the sake of illustrative clarity).

The prices show a considerable temporal as well as cross-sectional variation, depending on the origin as well as rice variety (indicated by line types, although labels are omitted for the sake of illustrative clarity).

For El Niño Southern Oscillation, we use weekly data on sea surface temperature anomalies, obtained from the Climate Prediction Centre of the National Oceanic and Atmospheric Administration, for the Niño3.4 region (5^{o}N—5^{o}S, 120^{o}W—170^{o}W) as a proxy for ENSO. The series are illustrated in the bottom panel of Figure 1. The shaded regions indicate "official" El Niño (shade of red) and La Niña (shade of blue) episodes, based on a threshold of 0.5 degree Celsius of the three-month running mean of SST anomalies (known as the Oceanic Niño Index) when the threshold is met for a minimum of five consecutive overlapping three-month periods. The sample covers several ENSO episodes, including the most notable El Niño event of the 21st century.

Empirical Framework

We consider two inter-related techniques here. First, we apply the local projections method of Jorda (2005) to generate impulse responses for up to 26-week horizons to illustrate changes in rice price growth after ENSO shocks. Second, we apply the direct forecasting method to assess the role of ENSO in predicting rice prices over the considered horizons. We describe these two methods below.

Local Projections

Impulse response analysis is a widely applied tool to gain insights about dynamic relationships among two or more potentially related variables. One way to illustrate the dynamic linkages among these variables is to directly project the effect of a (structural) shock to a desired horizon, following the local projections method put forward by Jorda (2005). Specifically, for a vector of variables, $\mathrm{x_t} = (\mathrm{x_{1,t}}, \dots, \mathrm{x_{n,t}})'$, an impulse response function is defined as follows:

$$IR(t, h, d_i) = E(x_{t+h}|\nu_t = d_i; \Omega_t) - E(x_{t+h}|\nu_t = 0_i; \Omega_t), \quad h = 1,2, \dots, \tag{1}$$

where under the assumption of quadratic loss, $\mathrm{E}(\mathrm{x_{t+h}}|\cdot)$ is the optimal (conditional) h-step-ahead forecast made in period t; Ω_t is the information set, ordinarily consisting of the vectors of lagged dependent variables; ν_t is a vector of reduced-form disturbances; and d_i is the i^{th} column of a matrix $\boldsymbol{D}$ that contains the relevant experimental shocks. For example, $\boldsymbol{D}$ can be the inverse of the lower triangular matrix $\boldsymbol{P}$ due to Cholesky decomposition of the reduced-from residual covariance matrix $\Sigma = \mathrm{E}(\mathrm{e_t e_t'})$, where the residuals are from:

$$x_t = \mu + B_{1x_{t-1}} + \cdots + B_{px_{t-p}} + e_t, \tag{2}$$

and where p is the autoregressive lag length.

Jorda (2005)'s local projections are, in effect, the multi-step variants of equation (2), such that:

$$x_{t+h} = \mu_h + B_{1,hx_{t-1}} + \cdots + B_{p,hx_{t-p}} + e_{t+h}, \; h = 0,1,2, \dots. \tag{3}$$

Notably, for h>0, $\boldsymbol{e_{t+h}}$ are likely serially correlated, even though $\boldsymbol{e_t}$ are not. Thus, heteroskedasticity and autocorrelation consistent standard errors are needed for inference.

The impulse responses, according to equation (1), from these local projections are:

$$IR_{LP}(t,h,d_i) = B_{1,hd_i},\ h = 0,1,2,..., \tag{4}$$

with the conventional normalization $B_{1,0} = I$.

Two practical comments, related to this method and relevant to the present study, are in order.[2] First, the autoregressive lag length, p, need not be the same across the set of local projections (indeed, as the horizon increases, the autoregressive lag length, determined by an information criterion, for example, will decrease). Second, the impulse responses for the variables in the system can be obtained separately for each equation.

In the current exercise, the bivariate vector is $x_t = (z_t, y_t)$, where z is the sea surface temperature anomaly, measured in degree Celsius, in the Niño3.4 region, and y is the log-differenced price series of a given rice variety. Assuming the weak exogeneity of z, the system of local projections, for h=0,1,2,…, is given by:

$$z_{t+h} = \alpha_{0,h} + \alpha_{1,h}z_{t-1} + \cdots + \alpha_{p,h}z_{t-p} + \varepsilon_{t,h} \tag{5}$$

$$y_{t+h} = \beta_{0,h} + \beta_{1,h}z_{t-1} + \cdots + \beta_{p,h}z_{t-p} + \gamma_{1,h}y_{t-1} + \cdots + \gamma_{p,h}y_{t-p} + \upsilon_{t,h} \tag{6}$$

where, for each h, p is selected using Schwartz Information Criterion (SIC). Of interest are the responses of price returns to an ENSO shock, which we obtain for horizons 1 through 26, for the 20 considered rice varieties. These impulse responses are illustrated in Figure 2. In each facet, the solid line indicates the mean impulse response of price returns to a one-standard-deviation ENSO shock (equivalent to approximately 0.2 degree Celsius); the dashed lines indicate 90 percent confidence intervals, and the shaded areas indicate 95 percent confidence intervals of the impulse responses. The facets are color-coded so that each color

[2] We refer the reader to Jorda (2005) for further details on the method.

represents prices from a given country; the abbreviated facet titles indicate the country and rice variety (see Appendix Table A1 for details).

Direct Forecasts

As noted earlier, the foregoing local projections framework lends itself to direct forecasting routine. As before, let y denote the log-differenced price series. Suppose in period t, using the information set consisting of the observed prices, $\Omega_t^0 = \{y_t, y_{t-1}, \dots\}$, we intend to make a forecast for period t+h. We can obtain an h-step-ahead direct forecast as follows:

$$\hat{y}_{t+h|t} = E(y_{t+h}|\Omega_t^0) = \hat{\beta}_{0h} + \sum_{j=1}^{p_h} \hat{\beta}_{jh} y_{t+1-j} \tag{7}$$

where $\hat{\beta}_{jh}$ j=0,…,p_h, are the parameter estimates from regressing y_t on $y_{t-h}, \dots, y_{t-h-p_h}$, where p_h is the maximum lag length selected in each horizon-specific regression using SIC.

Suppose we add the observed realizations of the ENSO variable to our information set, that is $\Omega_t^1 = \{y_t, y_{t-1}, \dots, z_t, z_{t-1}, \dots\}$. We can obtain a relevant h-step-ahead direct forecast as follows:

$$\tilde{y}_{t+h|t} = E(y_{t+h}|\Omega_t^1) = \tilde{\beta}_{0h} + \sum_{j=1}^{p_h} \tilde{\beta}_{jh} y_{t+1-j} + \sum_{j=1}^{p_h} \tilde{\gamma}_{jh} z_{t+1-j} \tag{8}$$

Having generated the pair of forecasts, one that uses information about ENSO and one that does not, we can examine their relative accuracy. If, on average, $\tilde{y}_{t+h|t}$ are more accurate than $\hat{y}_{t+h|t}$, we can state that ENSO helps predict the returns. In other words, ENSO causes the returns in Ganger (1969) sense.

To infer forecast accuracy, we first calculate the adjusted loss differentials:

$$d_{th} = \hat{e}_{t+h|t}^2 - \tilde{e}_{t+h|t}^2 + \left(\hat{y}_{t+h|t} - \tilde{y}_{t+h|t}\right)^2, \tag{9}$$

where $\hat{e}_{t+h|t}^2$ and $\tilde{e}_{t+h|t}^2$ are h-step-ahead forecast errors from models without ENSO (restricted model) and with ENSO (unrestricted model), respectively; the last component is an adjustment factor, which is needed here as the restricted model is nested within the unrestricted model (Clark and West, 2007). We then regress d_{th} on a constant. The test of Granger non-causality is equivalent to the one-sided t test that the estimated coefficient is not statistically significantly different from zero. Table 1 presents the results of this exercise across the considered 20 rice varieties and for up to 26-step-ahead forecast horizons. Where the reported test statistics are greater than 1.645 (one-sided 0.05 test), there is evidence that ENSO facilitates more accurate forecasts of rice price returns.

For inference, we need a sample of forecasts for each horizon, which we generate by applying the so-called rolling window pseudo forecasting routine. Specifically, we split the series into the in-sample and out-of-sample segments; we used the data from the in-sample segment to estimate the parameters of the restricted and unrestricted models given by equations (7) and (8); we then used these parameter estimates to generate up to 26-step-ahead direct forecasts; finally, we compared these forecasts with the actual realized values from the retained out-of-sample segment of the data. We set the size of the estimation window to approximately 75 percent of the length of the available time series. Thus, the first in-sample segment covers observations from the week of 27 June 2011 to the week of 1 April 2019, providing forecasts for weeks of 8 April 2019 through 23 September 2019; the second in-sample segment covers observations from the week of 4 July 2011 to the week of 8 April 2019, providing forecasts for weeks of 15 April 2019 through 30 September 2019; and so on for as long as the available data allows. As a result, we generated 105 pseudo out-of-sample forecasts for each considered horizon.

Discussion and Conclusion

The results of the impulse response analysis and multi-step forecast assessment, outlined in the previous section, present several features of interest, which we summarize below.

First, we find compelling evidence that Thailand long grain white rice prices and, especially, long grain glutinous rice prices react to ENSO shocks. For the considered long grain white rice varieties, a one standard deviation ENSO shock, equivalent to 0.2 degree Celsius, results in approximately 0.1 percent higher weekly returns over the duration of several months following the shock. For the long grain glutinous rice, the magnitude of the shock is larger (up to 0.3 percent growth in returns over the 12-to-24-week horizon after the shock) and more evident. The role of ENSO in price determination of these rice varieties is further justified by the improved forecast accuracy of their price returns due to ENSO. In the case of long grain white rice varieties, the ability of ENSO to help predict prices is manifested during the 16-to-20-week horizons, while in the case of glutinous rice, the improved forecasts, due to ENSO, are observed already after the fourth week, lasting up until the 18-week horizon.

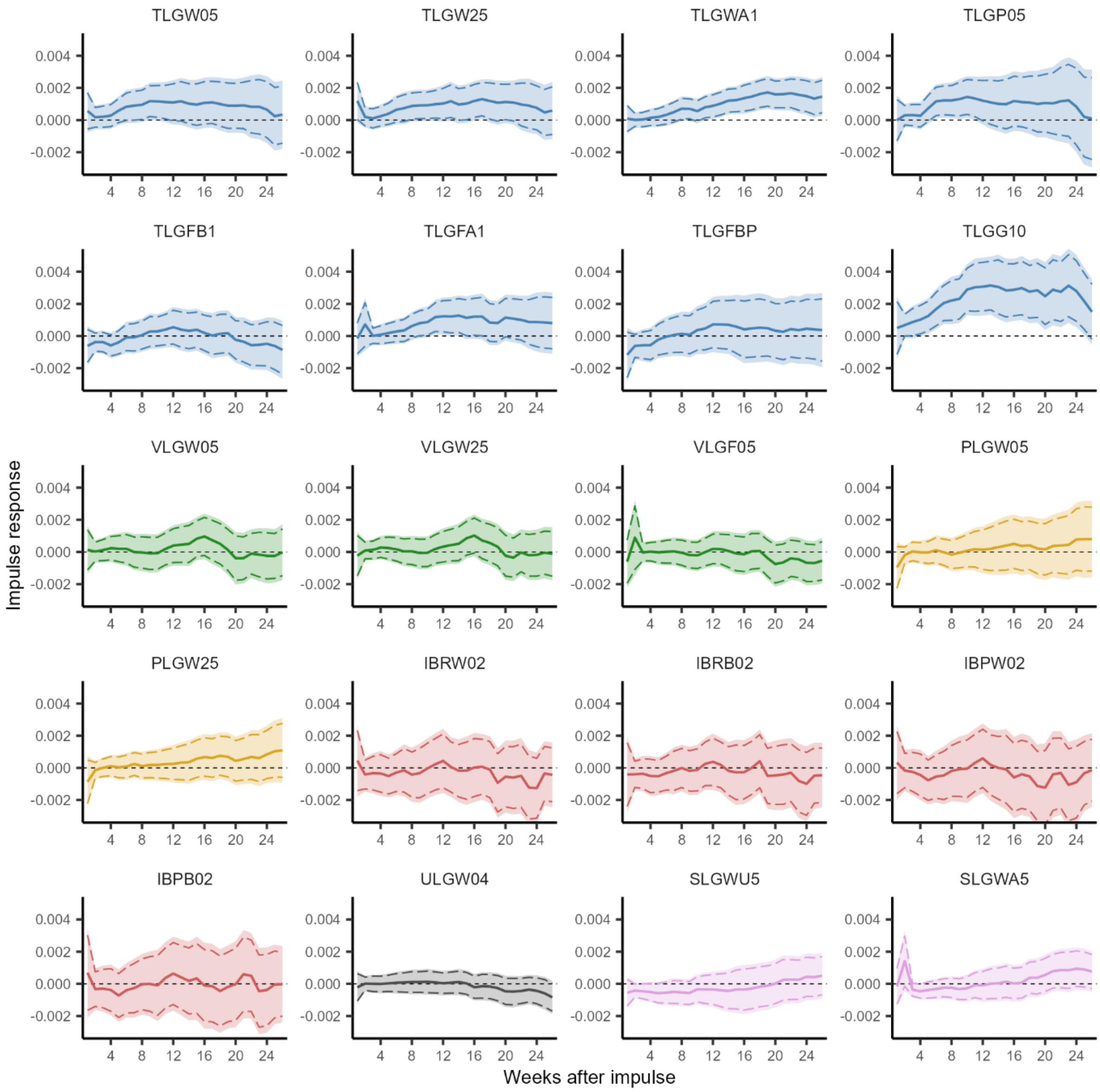

Figure 2: Impulse Responses from Local Projections.

Note: Each facet represents a rice variety and region; see Appendix Table 1 for details. The impulse-responses are obtained from Jorda (2005)'s local projections, where the impulse is equivalent to one-standard deviation shock from the `ENSO equation.' Solid lines represent mean impulse responses. Shaded areas represent 95% confidence intervals; dashed lines indicate 90% confidence interval. The

Table 1: Out-of-sample forecast accuracy

Origin	*Forecast horizon*																									
	1	*2*	*3*	*4*	*5*	*6*	*7*	*8*	*9*	*10*	*11*	*12*	*13*	*14*	*15*	*16*	*17*	*18*	*19*	*20*	*21*	*22*	*23*	*24*	*25*	*26*
Thailand																										
White 5% Broken	-0.73	-0.67	-0.65	0.11	0.11	0.04	0.17	0.23	-0.07	0.14	0.13	0.49	0.24	0.96	1.54	**2.07**	**2.04**	**2.04**	1.62	1.37	1.57	1.50	0.84	-0.19	-1.89	-2.27
White 25% Broken	-0.71	-0.67	-0.63	-0.19	-0.11	-0.24	0.28	0.28	0.29	0.34	0.27	0.62	0.28	1.18	1.39	**1.83**	**1.82**	**2.02**	**1.92**	1.57	**1.96**	**1.80**	1.36	0.76	-0.81	-0.11
White A1 Super 100% Broken	-0.84	-0.97	-0.62	-0.40	-0.33	-0.22	0.23	0.19	0.22	0.67	0.80	0.77	0.61	1.14	1.46	1.52	**1.78**	**2.21**	**1.96**	**1.77**	**1.83**	**1.92**	**1.77**	**1.65**	1.61	1.45
Parboiled Milled 5% Broken	-0.17	-0.41	-0.47	0.16	0.50	0.28	0.57	0.36	0.00	-0.18	0.06	0.54	0.43	1.20	**1.84**	**2.37**	**2.35**	**2.24**	**1.77**	1.59	1.57	**1.81**	1.10	0.18	-1.77	-1.85
Fragrant Hom Mali 100% Grade B	-1.19	-0.70	-0.85	-1.48	-1.68	-2.18	-2.11	-1.25	**1.72**	0.44	0.15	1.46	0.83	-0.07	0.74	-1.27	-1.70	-2.31	-1.31	-1.42	-0.80	-0.81	-0.64	-0.93	-0.73	-0.66
Fragrant Hom Mali A1 Super 100% Broken	-1.07	-1.01	-1.03	-1.05	-0.87	-0.95	-0.66	-0.43	-0.21	-0.09	-0.02	0.06	0.03	-0.17	0.16	0.23	-0.10	0.52	0.03	-0.33	-0.30	-0.32	-0.57	-0.54	-0.30	-0.61
Fragrant Pathumthani 100% Grade B	0.84	0.82	1.38	0.94	0.22	-0.20	-1.07	-1.01	-0.76	-0.26	-0.27	0.15	0.18	-0.05	-0.24	-1.06	-0.57	-0.13	-0.53	-1.19	-1.52	-1.21	-1.09	-0.48	-0.68	-1.24
White Glutinous 10% Broken	1.02	1.38	1.47	**2.09**	**1.93**	**2.01**	**2.36**	**2.17**	**2.33**	**2.37**	**2.23**	**1.90**	**2.00**	**1.79**	**1.99**	**1.84**	**1.98**	**2.07**	1.33	1.31	1.21	1.48	1.49	1.53	1.60	1.42
Vietnam																										
White 5% Broken	-0.91	-1.22	-1.88	-2.18	-0.91	-0.56	0.17	0.56	0.20	-0.58	-1.22	-1.88	-1.96	-2.39	0.51	1.17	-1.09	-1.82	-1.54	-1.44	-1.58	-1.51	-1.61	-1.62	-1.66	-1.92
White 25% Broken	-0.92	-0.99	-1.29	-1.72	-0.93	-0.50	0.13	0.47	0.26	-0.58	-1.32	-2.01	-1.98	-2.11	0.86	1.36	-1.08	-1.92	-1.47	-1.39	-1.73	-1.72	-1.63	-1.45	-1.72	-1.94
Fragrant 5% Broken	-0.52	-0.99	-1.39	-1.93	-0.84	-0.89	-0.77	0.17	0.03	-0.53	-0.80	-1.54	-2.52	-2.43	-2.16	-2.22	-2.32	-1.55	-0.56	-0.18	-0.37	-0.36	-0.33	0.26	0.11	0.05
Pakistan																										
White 5% Broken	1.36	-1.08	-1.10	-0.71	-0.90	-0.61	-0.80	-0.64	-0.62	-0.56	-0.43	-0.41	0.17	-0.20	-0.10	0.48	0.55	0.47	-0.95	-0.41	0.58	0.54	0.52	0.14	-0.22	0.53
White 25% Broken	-0.50	-0.70	-0.61	-0.59	-0.51	-0.67	-0.55	-0.62	-0.17	-0.34	-0.07	0.21	0.20	0.13	0.24	0.91	1.31	1.26	0.92	1.10	1.36	1.25	0.55	0.46	0.39	0.71
India																										
Basmati White 2%	0.84	0.56	0.23	0.22	0.44	-0.16	-0.48	-0.32	-0.02	-0.56	-1.66	-1.15	-1.84	-1.74	-1.16	-1.05	-0.72	-0.64	-0.55	-0.33	-0.36	-0.33	-0.02	0.05	-0.59	-0.04
Basmati Brown 2%	0.70	0.68	0.71	0.51	0.13	-0.16	-0.29	-0.25	0.12	-0.48	-1.90	-1.71	-0.64	-0.25	-0.46	-0.33	0.55	0.77	-0.56	0.29	-0.18	0.13	0.25	0.27	0.55	0.40
Basmati Pusa White 2%	-0.24	0.00	0.41	0.65	0.67	**1.84**	0.38	-0.98	-1.40	-1.07	-0.43	-0.49	-0.84	-0.56	-0.65	0.12	1.35	1.13	1.48	0.65	0.39	1.04	0.10	0.28	-0.31	-1.27
Basmati Pusa Brown 2%	-0.76	-1.71	-0.22	0.18	-0.04	0.81	-1.77	-1.14	-1.06	-0.90	-0.19	0.05	-0.14	-0.08	0.83	-0.30	0.98	-0.12	0.41	-0.62	-0.17	-0.22	-1.08	-0.39	0.09	-0.42
United States																										
U.S. No.2, 4% Broken	-2.38	-2.77	-3.08	-3.18	-3.10	-3.51	-2.54	-1.93	-2.76	-2.92	-4.00	-3.99	-2.68	-2.74	-4.14	-1.33	-2.04	-1.08	-0.66	-0.61	-0.51	-0.84	-0.46	-0.33	-0.18	-0.32
South America																										
(Uruguay) White 5% Broken	0.87	0.15	0.98	0.81	0.36	-0.06	-0.07	0.21	-0.67	-0.22	0.06	-0.03	0.15	-0.45	-0.29	-0.70	-0.94	-1.88	-2.07	1.02	**2.34**	**1.87**	1.43	**2.39**	**2.30**	**2.13**
(Argentina) White 5% Broken	0.33	-0.54	0.17	0.28	-0.27	-0.58	-0.61	-0.35	0.26	0.05	0.17	-0.13	-0.40	-0.11	0.82	0.20	-0.42	**1.76**	**1.67**	**2.11**	**2.25**	**2.25**	**2.47**	**2.00**	**2.01**	**2.17**

Note: The entries are the regression-based heteroskedasticity and autocorrelation consistent modified Diebold-Mariano test statistics (Diebold and Mariano, 1995; Harvey, et al. 1997) adjusted for nested models following Clark and West (2007). Values greater than 1.64 are statistically significant at 5% significance level (one-sided); for convenience, such values are given in boldface. The test statistics are based on loss differentials, obtained from a pair of forecasts for each considered horizon. The pseudo out-of-sample forecasts are generated using equal size rolling estimation windows of approximately 75 percent of the length of the series.

Second, we find some evidence that South American rice varieties also react to ENSO shocks. The dynamic pattern differs from that described above, however. For the two considered rice varieties, the returns first decrease then increase. The magnitude of the effect is not as pronounced as in the case of Thailand rice varieties, and ranges from negative 0.05 percent to positive 0.05 percent. While the impulse response functions show more apparent downward drift in the initial weeks after the shock, the forecast accuracy tests indicate the improved predictability of returns, due to ENSO, only at long horizons, starting from week 18 and onward.

Other considered price varieties show little market reaction to ENSO shocks. This can be due to a combination of factors. To begin, the South Asian rice producing regions are perhaps less affected by ENSO-related weather adversities than the Southeast Asian rice producing regions. Moreover, as also observed in Thailand fragrant rice varieties, it appears that the aromatic rice varieties are relatively less responsive to ENSO shocks, which may point to differences in market structure in these markets. The scope of the present study does not allow investigating this, of course, so we leave this note as a mere speculation.

In conclusion, our study unveils some linages between ENSO shocks and rice prices, which had been undetected by previous studies that relied on temporally more aggregated and geographically less diverse price series. This finding presents policy makers in the affected regions with an early warning tool to act upon in times of extreme ENSO events.

References

Bandumula, N. (2018). Rice Production in Asia: Key to Global Food Security. *Proceedings of the National Academy of Sciences, India Section B: Biological Sciences,* 88(4): 1323–1328.

Chen, B., and S. Saghaian (2016). Market Integration and Price Transmission in the World Rice Export Markets. *Journal of Agricultural and Resource Economics*, 41(3): 444–457.

Chulaphan, W., Chen, S., Jatuporn, C., and W. Huang (2013). Different Causal Relationships of Export Rice Prices in the International Rice Market. *American-Eurasian Journal of Agricultural & Environmental Sciences,* 13(2): 185–190.

Clark, T. and K. West (2007). Approximately Normal Tests for Equal Predictive Accuracy in Nested Models. *Journal of Econometrics,* 138(1): 291–311.

Diebold, F. and R. Mariano (1995). Comparing Predictive Accuracy. *Journal of Business & Economic Statistics,* 13(3): 253–263.

Fan, S., C. Chan-Kang, K. Qian, and K. Krishnaiah (2005). National and International Agricultural Research and Rural Poverty: The Case of Rice Research in India and China. *Agricultural Economics,* 33(s3): 369–379.

Ghoshray, A. (2008). Asymmetric Adjustment of Rice Export Prices: The Case of Thailand and Vietnam. *International Journal of Applied Economics*, 5(2): 80–91.

Granger, C. W. (1969). Investigating Causal Relations by Econometric Models and Cross-Spectral Methods. *Econometrica,* 37(3): 424–438.

Harvey, D., S. Leybourne, and P. Newbold (1997). Testing the Equality of Prediction Mean Squared Errors. *International Journal of Forecasting,* 13(2): 281–291.

Jamora, N., and S. von Cramon-Taubadel (2017). What World Price? *Applied Economic Perspectives and Policy*, 39(3): 479–498.

John, A. (2013). Price Relations Between Export and Domestic Rice Markets in Thailand. *Food Policy,* 42: 48–57.

Jordà, Ò. (2005). Estimation and Inference of Impulse Responses by Local Projections. *American Economic Review*, 95(1): 161–182.

Koizumi, T., G. Furuhashi (2020). Global Rice Market Projections Distinguishing Japonica and Indica Rice Under Climate Change. *Japan Agricultural Research Quarterly*, 54(1): 63–91.

Takahashi, K. and C. B. Barrett (2014). The System of Rice Intensification and Its Impacts on Household Income and Child Schooling: Evidence from Rural Indonesia. *American Journal of Agricultural Economics*, 96(1): 269–289.

Ubilava, D. (2018). The Role of El Niῇo Southern Oscillation in Commodity Price Movement and Predictability. *American Journal of Agricultural Economics*, 100(1): 239-263.

Wang, R., R. M. Rejesus, J. B. Tack, J. V. Balagtas, and A. D. Nelson (*2022*). Quantifying the Yield Sensitivity of Modern Rice Varieties to Warming Temperatures: Evidence from the Philippines. *American Journal of Agricultural Economics*, 104(1): 318-339.

Appendix

Table A1: Rice varieties used in the analysis

Origin and type	Code
Thailand, long grain white, 5% broken	TLGW05
Thailand, long grain white, 25% broken	TLGW25
Thailand, long grain white, A1 Super 100% broken	TLGWA1
Thailand, long grain parboiled milled 5% broken	TLGP05
Thailand, long grain fragrant Hom Mali, 100% grade B	TLGFB1
Thailand, long grain fragrant Hom Mali, A1 Super 100% broken	TLGFA1
Thailand, long grain fragrant Pathumthani, 100% grade B	TLGFBP
Thailand, long grain white glutinous, 10% broken	TLGG10
Vietnam, long grain white, 5% broken	VLGW05
Vietnam, long grain white, 25% broken	VLGW25
Vietnam, long grain fragrant, 5% broken	VLGF05
Pakistan, long grain white, 5% broken	PLGW05
Pakistan, long grain white, 25% broken	PLGW25
India, Basmati white, 2% broken	IBRW02
India, Basmati brown, 2% broken	IBRB02
India, Basmati Pusa white, 2% broken	IBPW02
India, Basmati Pusa brown, 2% broken	IBPB02
U.S., long grain No.2, 4% broken	ULGW04
South America (Uruguay), long grain white, 5% broken	SLGWU5
South America (Argentina), long grain white, 5% broken	SLGWA5